

## NEW SIZE NUMBER AND THE FRACTURE STATE OF CONCRETE STRUCTURE

V. TRAN TU  
*NCNST of Vietnam*

**ABSTRACT.** A new size number describing the fracture state of concrete structures is developed in which the structural size and the main fracture properties of concrete are dealt with. The relation between the fracture state of concrete beams loaded in bending and the newly proposed size number is presented graphically. The shape of the stress - crack curve, which is a typical property of most quasi-brittle composites like concrete, is found to be an important factor in determining the size number together with the fracture energy, the elastic modulus and the ultimate tensile strength of materials. The influence of the structural size on the fracture state is also graphically presented.

### 1. INTRODUCTION

As it has been empirically demonstrated that the state of the crack propagation (stable or unstable) in concrete structures strongly depends on the structural size, configuration and the fracture properties of materials. For structures made of the same material and with similar configuration, differing only in the structural size, the structures of smaller size seems to be more ductile as subjected to a load. The fracture state of concrete beams in three-point bending has been proved well by Carpinteri (1986), [1] using the energy brittleness number ( $S_E$ ) as

$$S_E = \frac{G_F}{bf_t} \quad (1.1)$$

In which the influence of the beam size and some material fracture properties as the energy fracture ( $G_F$ ) and the tensile strength ( $f_t$ ) on the fracture state are covered. It has been demonstrated graphically (Fig. 1) that the fracture mode changes from the more ductile state ( $S_E$  is higher) to the more brittle one ( $S_E$  is lower). However the number  $S_E$  does not deal with the influence of the stress - crack opening relation ( $\sigma - w$  relation) which is a typical property of concrete and most quasi-brittle composite materials. As it has been well known that this relation changes for different composition of concrete and it is proved to strongly influence the fracture parameters in concrete structures (Carpinteri et al., 1987; Duda and König, 1992; Roelfstra and Wittmann, 1986; Tran tu and Kasperkiewicz, 1994).

In the text the influence of the stress - crack opening curve on the fracture state of concrete structures is checked by theoretically analyzing the fracture state of concrete elements loaded in the uniaxial tension and in bending. The general equation describing the fracture state is found. From this equation the size numbers proposed by Carpinteri ( $S_E$ ), [1] and Hillerborg ( $b/\ell_{ch}$ ), [6] are obtained. A newly proposed size number is developed and it may be called the critical size of materials. The numerical analytic results of the fracture obtained using the fictitious crack model for beams in three-point bending have been proved to be good for determination of the fracture state by the new size number.

In order to follow the matters presented in the text, a new term called the shape index of  $\sigma - w$  relation ( $S_T$ ) proposed by Tran Tu and Kasperkiewicz (1994), [14] is presented briefly. It is defined as follows:

$$S_T = \frac{G_F}{f_t w_c} \quad (1.2)$$

We can consider some typical properties of the shape index  $S_T$ . Using Eq. (1.2), it may be said that  $S_T$  approaches infinity in case of elastic materials ( $w_c$  reduces to zero). For the plastic fracture materials  $S_T$  equals 1 (in this case  $G_F = w_c f_t$ ). With concrete when the  $\sigma - w$  curve is taken to be mono-straight  $S_T = 0.5$  ( $G_F = w_c f_t / 2$ ). From Eq. (1.2) we expect  $S_T$  to be one of the parameters determining the shape of the  $\sigma - w$  curve.

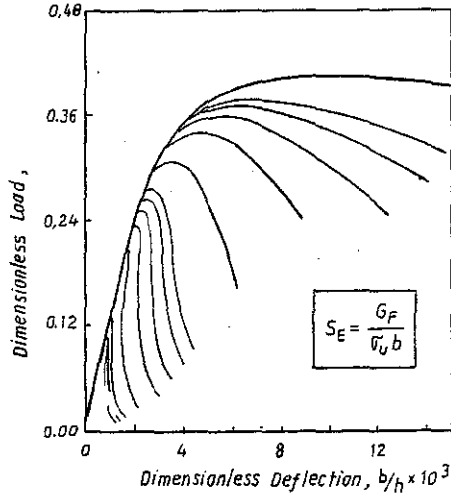


Fig. 1. The fracture state of beam in three-point bending and the energy brittle number  $S_E$  [2]

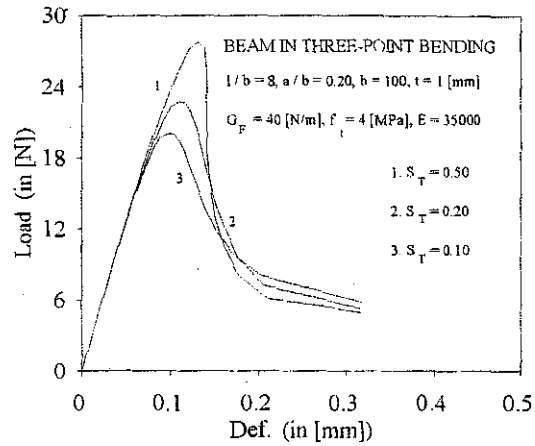


Fig. 2. The fracture state of beam in three-point bending depends on the shape of the  $\sigma - w$  curve

## 2. FRACTURE STATE OF CONCRETE STRUCTURES

According to Carpinteri (1990), [2] stable or unstable fracture state is defined by the slope of the post-failure branch of load-deflection diagram referring to the vertical direction. The following example shows that the size number  $S_E$  is insufficient to estimate the fracture state. Fig. 2 gives three load-deflection diagrams taken from numerical fracture analysis for notched beam in three-point bending with  $G_F = 40$  [N/m],  $f_t = 4$  [MPa],  $E = 35000$  [MPa] with  $S_T$  ranging between 0.10 and 0.5 (as shown in Figure). In this case the value  $S_E$  calculated from Carpinteri's proposal is constant:  $S_E = 10^{-4}$ . As it has been seen in Figure, fracture state depends on the shape of the  $\sigma - w$  curve.

At first, let us study an uniaxial tensile specimen, (Fig. 3) in which a part B is assumed to be very short so that its boundary displacement is to the crack opening displacement. The total displacement of a system composing of the testing machine and the specimen  $d$  is determined as

$$\delta = C_m P + \frac{L}{EF} P + w \quad (2.1)$$

where  $L$  and  $F$  are the length and cross-sectional area of the part A of specimen,  $E$  - elastic modulus,  $C_m$  - compliance of the test machine,  $P$  - tensile load and  $w$  - boundary displacement of the part B evaluated by the relation between the tensile stress and the crack opening displacement

$g(\sigma/f_t)w_c$ , that is the intrinsic fracture property of the material. In order to study the fracture state of the specimen, let us differentiate  $g$  with respect to  $P$  and denoting  $D_w = -\partial g/\partial(\sigma/f_t)$  as

$$\frac{\partial \delta}{\partial P} = C_m + \frac{L}{EF} - \frac{w_c}{f_t F_w} D_w \quad (2.2)$$

where  $F_w$  is the cross-sectional area at notch.

The fracture state of specimen is determined by the value  $\partial \delta/\partial P$ . The stable state occurs when  $\partial \delta/\partial P < 0$  and the unstable one when  $\partial \delta/\partial P \geq 0$ . Let us study the limiting state from the following

$$\frac{w_c}{f_t F_w} D_w = C_m + \frac{L}{EF} \quad (2.3)$$

The influence of the stiffness of a testing machine on the fracture state of a specimen is included in Eq. (2.2). With the machine controlled in loading well as in displacement, the first term in the right side of Eq. (2.2) can be neglected, we arrive at the following expression:

$$\frac{w_c}{f_t} D_w = \frac{LF_w}{EF} \quad (2.4)$$

From Eq. (2.4) we can derive the size numbers proposed by Hillerborg and Carpinteri assuming that the  $\sigma - w$  curve is a mono-straight, this means that  $D_w = -1$ , substituting  $G_F = w_c f_t/2$  and moving  $E$  to the left side, Eq. (2.4) becomes:

$$\frac{G_F E}{F f_t^2} = \frac{LF_w}{2F^2} \quad (2.5)$$

The term in the right side is the size number proposed by Hillerborg. Similarly, moving  $f_t$  to the left side of Eq. (2.4) to the right side, we get

$$\frac{G_F}{F f_t} = \frac{L f_t F_w}{2EF^2} = \frac{LW_c F_w}{2f_t F^2} \quad (2.6)$$

The right side of Eq. (2.6) represents the elastic strain energy stored in body divided by maximum tensile load and the energy brittleness number proposed by Carpinteri derived. The above has proved that use of the size numbers proposed by Hillerborg and Carpinteri for simulation of the effect of the size on the fracture parameters and fracture state is only an approximation. As was shown clearly in Fig. 2. Previous investigations (Hillerborg 1987, [7]; Carpinteri 1990, [2]; and Liang 1992, [9]) proved that the maximum load reached for the crack opening displacement about 1/3 to 1/2 of  $w_c$ . Therefore in order to study the fracture state, the value  $D_w$  is taken in this range. As it has been seen in Fig. 3b,  $D_w$  increases with decreasing the shape index  $S_T$ , approximate replacement of  $D_w = 1/S_T$  in Eq. (2.4) we arrive at the following equation

$$\frac{EG_F}{f_t^2 S_T^2} = \frac{LF_w}{F} \quad (2.7)$$

which, the ratio  $L/F$  represents the slender and  $F_w/F$  represents the notched length of a specimen. The term in the left side of Eq. (2.7) is a function of the fracture properties, on the other hand the term on the right side is a function of the characteristic size of the specimen. Taking the left side of Eq. (2.7) to be a term having the dimension  $[L]$  and denoting  $L_s$  as

$$L_s = \frac{G_F E}{(f_t S_T)^2} \quad (2.8)$$

The above results are obtained from the uniaxial tensile specimen, we need to know how they behave in elements loaded in bending. Let us assume that a notched beam subjected to bending

load  $P$ , notched length is  $a$ , span and depth of the beam is  $\ell$  and  $b$  respectively, length of the fracture process region is  $\ell_c$ , cohesive forces is  $P_c$ . The deflection  $\delta$  at the mid-span of the beam is determined from the following equation:

$$\delta = C_m P + C_2 P + C_3 P \quad (2.9)$$

where  $C_m$  is the compliance of the test machine,  $C_2$  and  $C_3$  - compliances of the specimen caused by the action of  $P$  and  $P_c$  respectively. The value of  $P_c$  is determined from Fig. 4 by putting  $\ell_F = \ell_c/b$  and  $z = x/b$ :

$$P_c = \int_0^{\ell_F} f(w/w_c) f_t b dz \quad (2.10)$$

in which  $x$ -axis coincides with the crack growing direction and a function  $\sigma/f_t = f(w/w_c)$ .

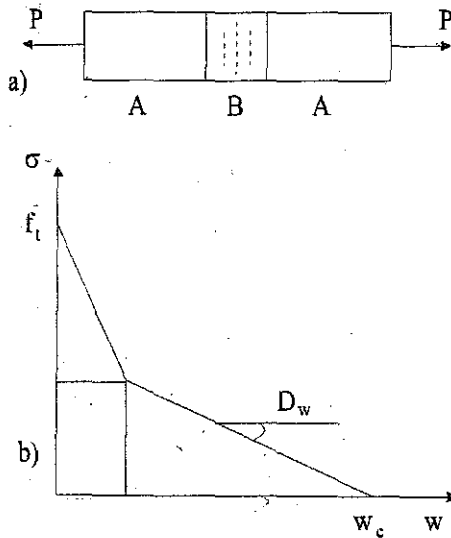


Fig. 3. A specimen loaded in tension and a bilinear diagram of the  $\sigma - w$  curve

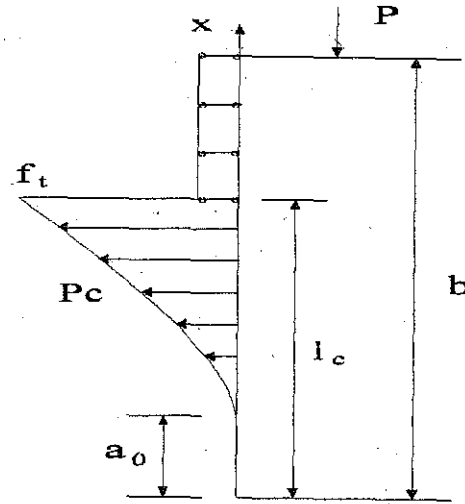


Fig. 4. A specimen loaded in bending and the distribution of cohesive forces

The value  $w$  is determined by the superposition of  $P$  and  $P_c$ :

$$w = C_4 P + C_5 P_c \quad (2.11)$$

where,  $C_4$  and  $C_5$  are compliances of the specimen in different cases of the studied point. Derivative  $\delta$  with respect to  $P$  and substituting (2.10), (2.11) into (2.9):

$$\frac{\partial \delta}{\partial P} = C_m + C_2 + C_3 \frac{\int_0^{\ell_F} C_4 dz}{\frac{w_c}{f_t b f(w/w_c)} - \int_0^{\ell_F} C_3 dz} \quad (2.12)$$

putting:

$$A = \int_0^{\ell_F} C_4 dz = A\left(\frac{a}{b}, \frac{\ell_c}{b}\right), \quad D = \int_0^{\ell_F} C_5 dz = D\left(\frac{a}{b}, \frac{\ell_c}{b}\right)$$

we derive the following formula:

$$\frac{1}{b} \frac{w_c}{f_t} D_w = \frac{C_3}{C_2} A - D \quad (2.13)$$

The left side of Eq. (2.13) similar to Eq. (2.4) is  $L_S$ , whereas the length of the fracture process zone has a functional relation with  $L_S$ , formally we can derive an expression as

$$\frac{EG_F}{(f_t S_T)^2} = \beta \left( \frac{a}{b}, \lambda, \lambda_p \right) b \quad (2.14)$$

where  $\lambda$  is the slender of beam and  $\lambda_p$  is a coefficient depending on the loading position.

Again we can see that the term in the left side of Eq. (2.14) is  $L_S$ , Whereas the right side only describes the dependence of the beam size on the loading condition. The term  $L_S$  is described by Eq. (2.8) and depends only on the intrinsic fracture properties of materials. Remembering that Eqs (2.4) and (2.14) express the limiting fracture state,  $L_S$  may thus be called the critical size of materials. As it has been seen in Fig. 5 the fracture state of a beam depends on the critical size of materials ( $L_S/b$  changes from 1.75 to 26.25).

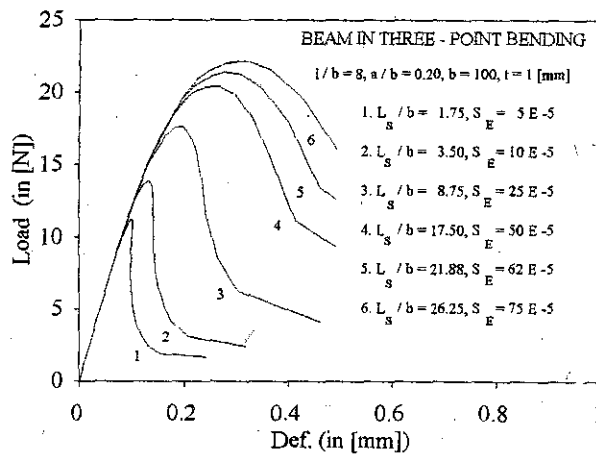


Fig. 5. The dependence of the fracture state of the critical size of concrete

### 3. PRESENTATION OF THE FRACTURE STATE IN NOTCHED BEAMS

#### 3.1. Numerical experiment

Important in the fictitious model for creating the cohesive forces and controlling them in the crack propagating process. The cohesive forces are calculated by steps based on the stress-crack opening relation. This relation were formulated by many researches such as Reinhardt (1984), [11]; Gopalratnam and Shah (1985), [5]; Cornelissen et al. (1987), [3] and Tran Tu and Kasperkiewicz (1994), [14]. As it is replaced by multi-linear diagrams as by Hillerborg et al. (1976), [6]; Peterson and Gustarsson (1981), [10]; Roelfstra and Wittmann (1986), [12]; Carpinteri (1987), [1]; etc. As it has been proved by Tran Tu and Kasperkiewicz (1994), [14] that the load-deflection diagrams for beams in bending obtained by applying the equations of Cornelissen et al., Gopalratnam and Shah, Tran Tu and Kasperkiewicz and the consistent bilinear diagrams, are rather similar. In this text Equation describing the stress-crack opening curve proposed by Tran Tu and Kasperkiewicz (1994) is used:

$$\frac{\sigma}{f_t} = (1 - A)(1 - x^k) + A(1 - x)^{1/k} \quad (3.1)$$

$$x = \frac{w}{w_c}, \quad k = \frac{S_T}{1 - S_T}$$

where the coefficient  $A$  is chosen to be 0.5. The change of  $A$  may be offset by changing the shape index  $S_T$  which does not have much influence on the obtained results. The use of Eq. (3.1) is convenient for covering the influence of the stress-crack opening curve on the fracture parameters in concrete structures. In which a change is only in the shape index  $S_T$  that is considered to be the intrinsic fracture property of concrete.

Numerical approach can be presented in brief as follows:

1) Calculating the load where the micro crack starts developing. The length of the real crack is the notched length. The fracture criterion of the critical stress intensity factor is employed.

2) Calculating the crack extension, the maximum main stress criterion is used. The fictitious crack length is assumed to increase by steps until the total length of the real crack and the fictitious crack reaches the crack ligament. The cohesive forces are calculated according to the  $\sigma - w$  relation by iteration. They are controlled by the critical deviations of two neighboring steps, not larger than the specific value (it is specified here about 0.01 [N]). It has been proved (Tran Tu and Kasperkiewicz, 1994) that the load-deflection diagrams will be discrepant if the shape of the  $\sigma - w$  curve is missing.

### 3.2. Fracture state of concrete notched beams in bending

In this chapter the illustrations on the fracture state in the concrete notched beams in three-point bending is presented. It includes the influence of the material fracture properties and the beam depth through the critical size to beam depth ratio ( $L_S/b$ ).

1) Arrangements are made, that include the change of the fracture energy  $G_F$  from 20 [N/m] to 180 [N/m] and the shape index  $S_T$  from 0.1 to 0.9. the unchanged factors are the tensile strength  $f_t = 4$  [MPa], the elastic modulus  $E = 35000$  [MPa], the beam sizes: depth  $b = 100$  [mm], span  $\ell = 800$  [mm], the thickness of unit is chosen. Fig.6 is plotted for  $G_F = 20 - 180$  [N/m] and  $S_T = 0.3$ . The ratio  $L_S/b$  and the energy brittleness number  $S_E$  are calculated and presented in the figure. In this case we can see that the fracture state becomes more ductile with the increase of the  $L_S$  and  $S_E$  similar to the results obtained by Carpinteri (1990).

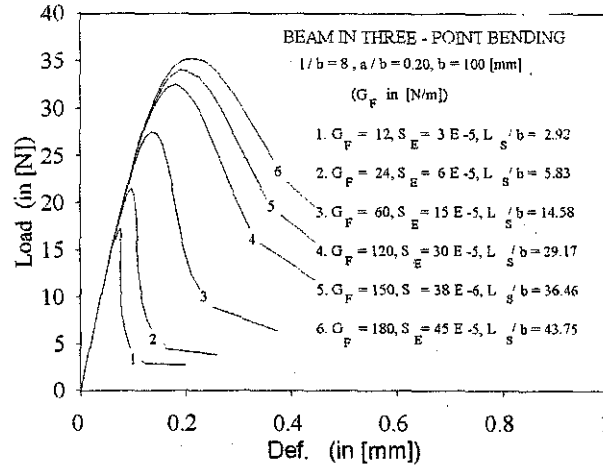


Fig. 6. The dependence of the fracture state on the critical size with the changing fracture energy

The change of the shape index  $S_T$  is presented in Fig.7. The values  $L_S/b$  and  $S_E$  are also calculated and presented in graphs. We can see that the fracture state becomes more brittle as the value  $S_E$  increases contrarily to the conclusion of Carpinteri. In this case the value  $L_S$  decreases in accordance with the theoretical prediction.

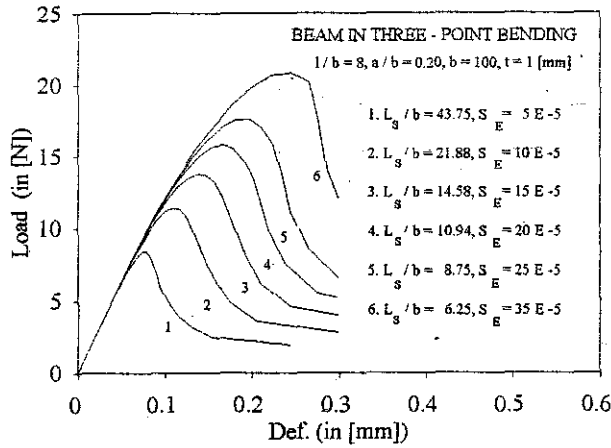


Fig. 7. The dependence of the fracture state on the critical size with the changing shape of the  $\sigma - w$  curve

2) In the second case the dependence of the fracture state on the  $L_S$  with the change of elastic modulus of concrete is studied. Three load-deflection diagrams are plotted with the same  $G_F = 80$  [N/m],  $f_t = 4$  [MPa] and  $w_c = 0.05$  [mm]. The values of the elastic modulus are shown in Fig. 8. We can see clearly in the figure that the fracture state becomes more brittle with the increase of elastic modulus.

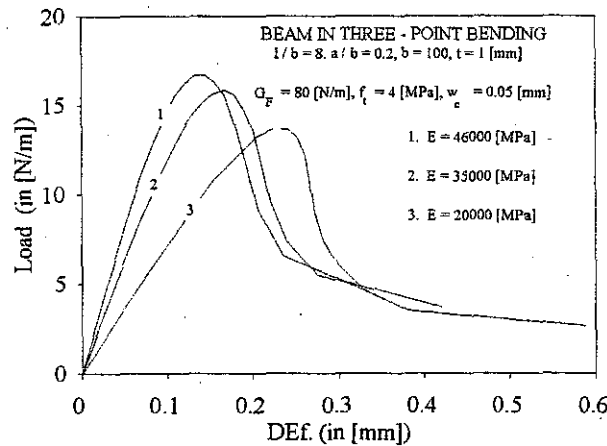


Fig. 8. The dependence of the fracture state on the elastic modulus of concrete

3) The last, the effect of the change in the beam depth is studied and otherwise unchange. This is a case that was noted by many researches. The change of beam depth between 100 [mm] and 400 [mm], the fracture energy of 80 [N/m] and  $S_E$  of 0.4 are chosen. We can see clearly that the fracture state becomes more brittle with increasing beam depth (Fig. 9).

#### 4. CONCLUSION

The critical size  $L_S$  may be considered as the intrinsic fracture property of concrete and similar materials. It characterizes the fracture state (stable or unstable) of concrete structures.

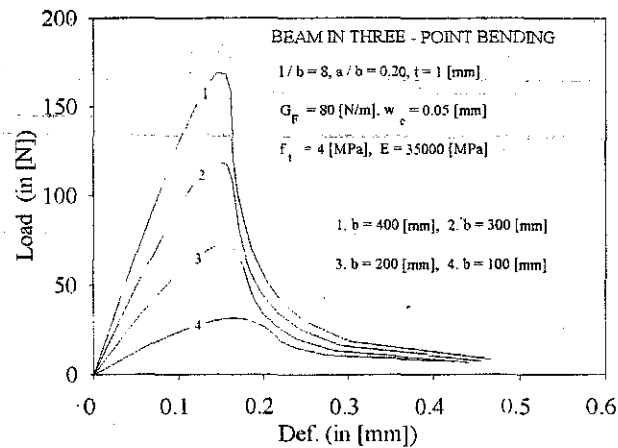


Fig. 9. The fracture state changes in accordance with the changes of beam depth

**Acknowledgement.** The writer kindly appreciates the supports given by Prof. A. M. Brandt and Prof. J. Kasperkiewicz. The help from other members at the Strain Section is also acknowledged.

#### REFERENCES

1. Carpinteri A., et al. Numerical simulation of concrete fracture through a bilinear softening stress-crack opening displacement law, in *Fracture of concrete and rock*, ed. S. P. Shah and S. E. Swartz, Houston, 131-141, 1987.
2. Carpinteri A. Nonlinear phenomena associated with fracture in strain-softening materials, in *Nonlinear fracture mechanics*, ed. M. P. Wnuk, Springer-Verlag-Wien-NewYork, 61-122, 1990.
3. Cornelissen H. A. W. et al. Experiments and theory for the application of fracture mechanics to normal and lightweight concrete, *J. Engng Mech.* Vol. 113, No 3, 1987.
4. Duda H. and König G. Stress-crack opening relation and size effect in Concrete, in *Applications of fracture mechanics to reinforced concrete*, ed. A. Carpinteri, Elsevier applied Science, 45-61, 1992.
5. Gopalaratnam V. S. and Shah S. P. Softening response of plain concrete in direct tension, *ACI J.* Vol. 82, 310-324, 1985.
6. Hillerborg A., Modeer M. and Petersson P. E. Analysis of crack formation and crack growth in Concrete by means of fracture mechanics and finite elements, *J. Cement and Concrete Research*, Vol. 6, 773-782, 1976.
7. Hillerborg A. Constitutive models, Chapter 4.2: Discrete crack approach, in *fracture mechanics of concrete applications - Part A*, RILEM TC 90-FMA, 1987.
8. Hordijk A. Material properties, Chapter 3.1.1: Tension, in *fracture mechanics of concrete applications - Part A*, RILEM TC 90-FMA, 1987.
9. Li Y. -N. and Liang R. Y. Stability theory of cohesive crack model, *J. Engng Mech.*, Vol. 118, 587-603, 1992.
10. Petersson P.E. and Gustarsson P. J. A model for calculation of crack growth in concrete-like materials, in *numerical method in fracture mechanics*, ed. D. R. J. Owen and A. R. Luxmoor, Swansea 707-719, 1981.



11. Reinhardt H. W. Fracture mechanics of an elastic softening material like concrete. Heron, Vol. 29, 1-42, 1984.
12. Roelfstra P. E. and Wittmann F.H. Numerical method to link strain softening with failure of concrete, in fracture toughness and fracture energy of concrete, ed. F. H. Wittmann, 127-139, 1986.
13. Tommaso A. D. Structural applications, Chapter 5.1: General remarks, in fracture mechanics of concrete applications - Part B, RILEM TC 90-FMA, 1987.
14. Tran Tu V. and Kasperkiewicz J. The relationship between stress and crack opening in concrete, Proc. Int. Symp. Brittle Matrix Composites 4, September 13-15, 1994, ed. A. M. Brandt, V. C. Li, I. H. Marshall, IKE and Woodhead publ. Warsaw, 1994.

*Received December 28, 1995*

### HỆ SỐ ẢNH HƯỞNG KÍCH THƯỚC MỚI VÀ TRẠNG THÁI PHÁ HỦY CỦA KẾT CẤU BÊ TÔNG

Một hệ số ảnh hưởng kích thước của kết cấu bê tông được phát hiện trong đó kích thước của kết cấu và tính chất phá hủy của vật liệu được thể hiện trong công thức. Bằng đồ thị, tác giả chứng minh được sự phụ thuộc lớn của trạng thái phá hủy của dầm bê tông chịu uốn ba điểm vào số kích thước mới này. Hình dạng của đường cong ứng suất - độ mở vết nứt ( $\sigma - w$ ), đây là một tính chất điển hình của vật liệu bê tông và các vật liệu composite tương tự, đã được chỉ ra như là một yếu tố đặc biệt quan trọng ảnh hưởng đến trạng thái phá hủy. Ngoài ra vai trò quan trọng của các tính chất phá hủy khác của bê tông như mô đun đàn hồi  $E$ , năng lượng phá hủy  $G_F$  cũng được thể hiện từ kết quả phân tích phá hủy.

### DÉTERMINATION DE L'INFLUENCE DU TRAJET ...

*(tiếp theo trang 39)*

7. Hill R. (eds), 1950, Mathematical theory for plasticity, Clarendon press, Oxford.
8. Hage Chehade I. Simulation de l'emboutissage de déformation sur les courbes limites d'emboutissage à striction et à rupture. Thèse Doct. INSA Lyon 1990, 163p.

*Received January 3, 1996*

### NGHIÊN CỨU ẢNH HƯỞNG CỦA QUỹ ĐẠO BIẾN DẠNG ĐẾN ĐƯỜNG CONG GIỚI HẠN HÌNH THÀNH

Mục đích nghiên cứu ở đây là dự đoán ảnh hưởng của quỹ đạo biến dạng đến đường cong giới hạn hình thành, từ biểu đồ ứng suất giới hạn. Chúng ta sẽ nghiên cứu quỹ đạo cấu tạo từ hai đoạn thẳng tương ứng với các giai đoạn: kéo đúng tâm - dần đều hoặc ngược lại.